

## STRUCTURAL COLORS OF SELF-SIMILAR NANOPATTERNS

MELUZÍN Petr<sup>1,\*</sup>, HORÁČEK Miroslav<sup>1</sup>, KRÁTKÝ Stanislav<sup>1</sup>, KOLARŽÍK Vladimír<sup>1</sup>

<sup>1</sup> *Institute of Scientific Instruments of the CAS, Brno, Czech Republic, EU*

\* [petr.meluzin@isibrno.cz](mailto:petr.meluzin@isibrno.cz)

### Abstract

E-beam lithography is a flexible technology for various diffraction gratings origination. The e-beam patterning typically allows for the creation of optical diffraction gratings in the first diffraction order. However, the very high resolution enables also the patterning of structures providing the zero-order diffraction. Recently, we presented a work on the structural colors of metallic layers covering both regular-line structures and CGH (computer generated hologram) structures. This work presents a study dealing with zero-order diffraction structures with self-similar properties. The practical part of the work is focused on two aspects: design parameters and technological issues. Variations in design parameters include the tone of the structure (positive or negative), the density of filling, the filling factor, and the depth of the structures. The achieved gamut of colors may be primarily extended by the proper selection of metal deposition technology and its parameters, and further by the proper selection of the metal and the thickness of its layer; these are the technological issues.

**Keywords:** E-beam writer, nano patterning, self similarity, diffraction grating

### 1. INTRODUCTION

Recently, we presented a study on structural colors of metallic surfaces [1]. Both the structural colors and the asymmetric diffraction gratings belong to well-known strong security features of diffractive optically variable image devices [2]. Within the study on e-beam benchmarking patterns [3], we also presented one particular diffractive arrangement based on a quasi regular filling of a given area by the filling of elementary diffraction entities; this nature inspired approach uses the prosperous Vogel's model [4] of sunflower seed arrangement.

This contribution deals with zero-order diffraction structures that embody self-similar properties of the visible diffraction pattern. Sample planar relief structures are prepared using the Gaussian type e-beam pattern generator Vistec EBPG5000plusES. The finer is the patterned structure the better is the choice of the Gaussian type generator over the one with the shaped beam [5]. Alternatively, a combined exposure using both types of pattern generators (the Gaussian type for finer parts and the variable shaped type for coarser parts) represents an interesting option.

### 2. METHOD

Proposed arrangements of optical elements are described by two models. The first model defines coordinates of individual optical elements; this model is derived from a simple Vogel's model [4]. This model is for the purpose of simplicity two dimensional, the positions of a set of  $k$  optical elements arranged in a planar circular area are expressed in polar coordinates  $(r_k; \theta_k)$  according to equation (1). Here, the constant  $c$  is a main radial scale factor that basically defines the distance between adjacent elements. Homogeneous intensity of the optical element filling is ensured by selecting the exponent  $q = 2$ . Larger value of  $q$  makes the filling successively denser in the areas far from the central point (pole of the model), i.e. for larger value of  $k$ . Angular dependency of the optical element filling is derived from the angular constant  $\theta_0$ , which can be positive (CCW model) or negative (CW model); this constant should be an irrational number which has no good rational approximations [6]; usually, the appropriate value that fulfills this requirement is a golden angle -  $\pi \times (3 - \sqrt{5})$  in radians or approximately 137.5 degree.

$$\{r_k; \vartheta_k\} = \{c \cdot k^{1/q}; k \cdot \vartheta_0\} \quad (1)$$

The second model is a seed model that defines the shape and size of each seed (i.e. each optical element). Within this contribution we use the same cylindrical shape of each optical element, according to equation (2). The radius  $\rho_k$  of each micro cylinder is derived from the scale factor  $c$  and from the filling factor  $FF$ . The filling factor of 50 % means that one half of the total circular area populated by optical elements is formed by the sum of all individual element areas, while the other half represents the surrounding space. The height  $h_k$  of each micro cylinder is kept constant over the whole circular area. The numerical value of  $h_k$  depends on the physical realization, in our case it is related to a particular exposure dose  $D$ .

$$\{\rho_k; h_k\} = \{c \cdot \sqrt{FF}; h_D\} \quad (2)$$

The equation (2) is valid for any micro element shape with a circular base (cone, sphere). Alternatively, the square shape may be used (for micro objects in the shape of cube, cuboid, prism or pyramid). Then the micro object size  $\rho_{sq}$  is given by equation (3). Similar relations can be found for other shapes of the micro object base.

$$\rho_{sq} = c \cdot \sqrt{\pi \cdot FF} \quad (3)$$

There is a limit of the filling factor when the adjacent seeds (of the fixed size and shape) start to overlap. This limit depends on the shape of the seed base. The limit value of the filling factor for the circular base ( $FF_{c,max}$ ) and for the square base ( $FF_{sq,max}$ ) are described by equations (4) and (5) respectively; these values are derived from the minimum distance between seeds in the given coordinate model -  $\Delta_{min} = c \times \sqrt{\pi} \times \sqrt{fm}$ . Here, the constant  $fm$  is an arithmetic mean value of  $\Phi$  and  $\Phi^1 - \Phi = (\sqrt{5} + 1) / 2$ . Numerically, the values of maximum filling factor are  $FF_{c,max} \sim 70.21\%$  and  $FF_{sq,max} \sim 44.72\%$  (in fact, in the close vicinity of the pole these values are slightly different).

$$FF_{c,max} = \frac{\Delta_{min}^2}{4 \cdot c^2} \quad (4)$$

$$FF_{sq,max} = \frac{\Delta_{min}^2}{2 \cdot \pi \cdot c^2} \quad (5)$$

The density of optical element filling is practically constant, however there exists a small variation of distance between adjacent elements. This variation is hardly observable directly, but it is the origin of locally slightly different arrangement that may create differently visible colors of zero-order diffraction order. Moreover, these variations have a partial self-similarity property; the characteristic visible pattern is repeated with the increasing size from the pole of the model toward its perimeter.

### 3. EXPERIMENT

We prepared a testing set of small planar relief structures in order to validate the presented concept. The testing sample was patterned using the e-beam writer Vistec EBPG5000plusES (Gaussian type, with electron energies of 50 and 100 keV respectively). A thin layer of PMMA resist (thickness  $t_{PMMA} > 1000$  nm) was deposited on a 4-inch silicon wafer by the spin coating method.

**Table 1** Parameters of the positive-tone testing patterns (values of the filling factor  $FF$  [%] and the scaling factor  $c$  [nm], the resolution factor  $res = 1$  nm for all variants)

	variant						
	1	2	3	4	5	6	7
$FF$ [%]	50	50	50	50	50	50	50
$c$ [nm]	280	320	360	400	450	500	600
	variant						
	8	9	10	11	12	12	14
$FF$ [%]	60	60	60	60	60	60	60
$c$ [nm]	280	320	360	400	450	500	600
	variant						
	15	16	17	18	19	20	21
$FF$ [%]	70	70	70	70	70	70	70
$c$ [nm]	280	320	360	400	450	500	600

**Table 2** Parameters of the negative-tone testing patterns (values of the filling factor  $FF$  [%], the scaling factor  $c$  [nm] and the resolution factor  $res$  [nm])

	variant							
	22	23	24	25	26	27	28	29
$FF$ [%]	50	50	50	50	60	60	60	60
$c$ [nm]	600	600	600	600	600	600	600	600
$BSS$ [nm]	10	20	50	1	10	20	50	1

**Data preparation.** Each test variant is composed of a large number of elementary optical elements, the number is in order of  $10^7$  depending on the scale parameter  $c$ . Testing data are composed of two sets: 126 positive variants and 48 negative variants (see the layout in **Figure 2**). The positive variants have cylindrical micro holes (the area of the elements was exposed) while the negative variants have cylindrical micro pillars (the surrounding area of the elements was exposed). Parameters of the positive-tone variants are summarized in **Table 1**; parameters of the negative-tone variants are listed in **Table 2**. Size of each positive variant is 2.5 mm; size of each negative variant is 1.0 mm (these negative variants require much longer exposure time).

**Exposure and development.** A positive resist PMMA was used for the recording, the exposure dose  $D$  range from 100 to 200  $\mu\text{C}/\text{cm}^2$  (variants denoted A to F in **Figure 1**). An important factor that influences both the fineness of individual seeds and the writing speed is the resolution  $res$  of individual spot positions. While the  $res$  factor was set to 1 nm for all positive-tone variants, the negative-tone variants have a variable  $res$  factor, see details in **Table 2**. A proper care of proximity effect handling was necessary [7]. The exposed pattern was developed by n-amyl-acetate (nAAc). The planar relief structure was checked by optical microscope and the relief depth was checked using SPM (scanning probe microscopy). The relief depth  $t_{rel}$  varies according to the exposure dose in the range 100-450 nm. None variant was developed to the bottom of the resist layer.

**Metallization.** Two similar samples were realized as previously described. After the resist development process, each sample was finished with a different kind of metallization. The first sample of the planar relief structure was sputtered by a silver layer with the thickness  $t_{Ag} \sim 100$  nm. The sputtering process has quite isotropic characteristics. The second sample was metalized by vapor deposition: a thin aluminum layer with the thickness  $t_{Al} \sim 40$  nm; the vapor deposition process has more anisotropic character than the sputtering.

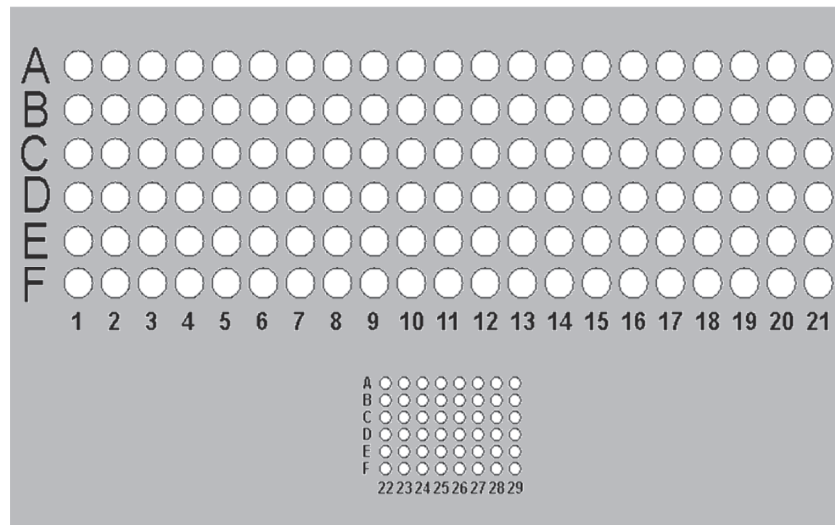


**Figure 1** Layout of the tested pattern:  
126 positive-tone variants and 48 negative-tone variants

#### 4. RESULTS AND DISCUSSIONS

Results of the sample preparation procedure are depicted in **Figure 2**. The mode of metallization has a visible impact on the color palette; generally, the variants of the sample covered by vapor deposited Al layer are darker and less pronounced. Within each of the samples the dependency of the color on the technology parameters (scaling parameter  $c$ , filling factor  $FF$ , exposure dose  $D$ ) is validated. The robustness of the technology process was verified by the realization of the third sample (an equivalent to the sample 2), the color palette of both samples is practically indiscernible.



**Figure 2** The palette of 126 positive-tone variants and 48 negative-tone variants:  
sample 1 metalized by Al vapor deposition (a);  
sample 2 metalized by Ag sputtering (b)

**Figure 3** shows the micro photo (magnification 50 $\times$ ) of one selected variant (D05) from both testing samples. Microstructures are characteristic by zero-order diffraction pattern which is of a different kind than the first order diffraction pattern presented in [3]. Labeled radii of successive blue rings in **Figure 3b** are approximately 52; 90; 143; 229; 357 and 589 microns, respectively. The mean ratio of two successive radii in this sequence is 1.626 that seems to be quite close to the ratio of 1.618.

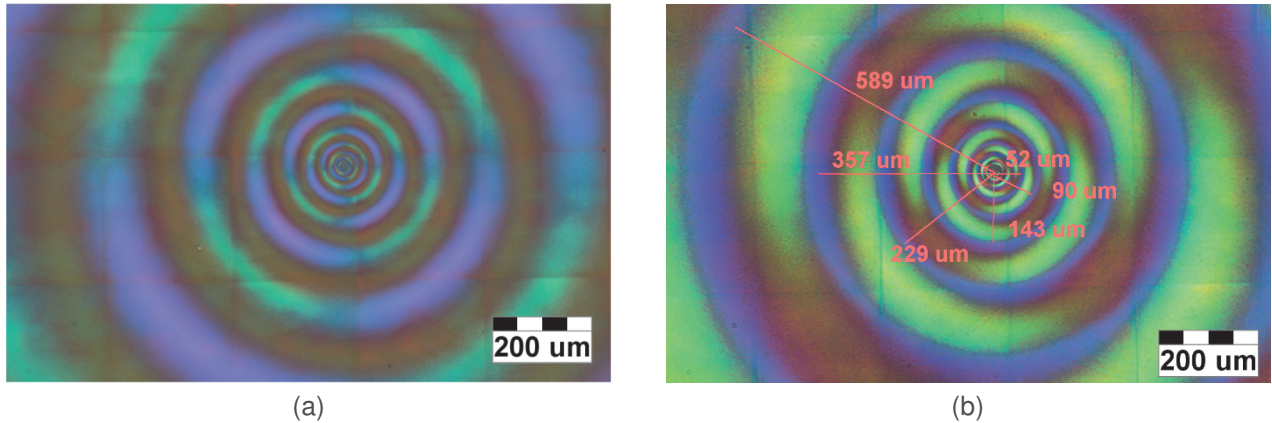


**Figure 3** Micro photo of one selected variant (D05): sample 1 (a); sample 2 (b); see text for details

Observations of scanning electron microscope (SEM) images indicate that the exposure dose  $D$  has an impact on both the aspect ratio (the ratio of the structure depth and the distance between adjacent elements) and the filling factor (the sum of individual elements area within a given region and the area of this region). **Figure 4** shows SEM images of two selected variants of the negative-tone testing patterns from sample 1 (with vapor deposited Al layer).

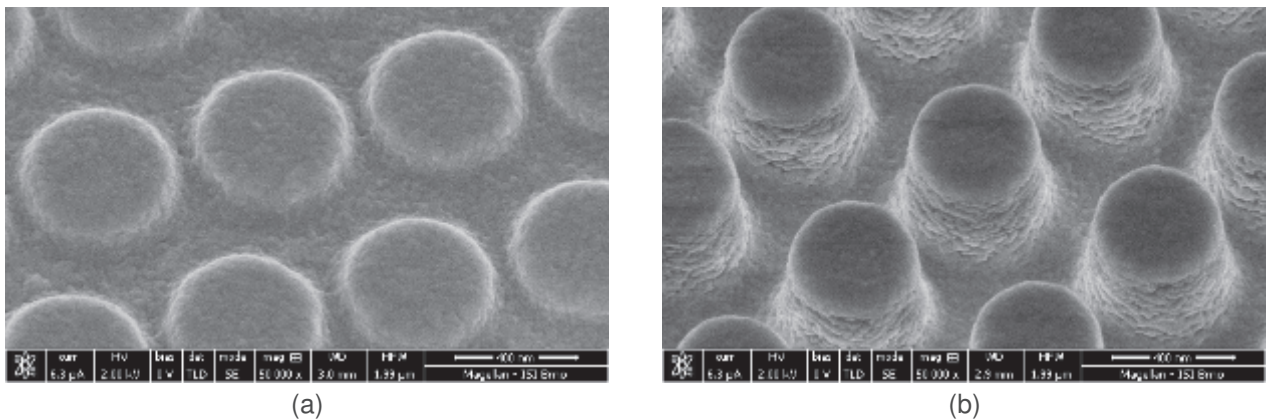


**Figure 4** SEM images of the negative-tone testing patterns, sample 1 with vapor deposited Al layer: variant A22 (a); variant F22 (b)

The similar color palette can be observed by the naked eye (or by photographic camera) and by the optical microscope (magnification 50 $\times$ ). We prepared an algorithm that enables the conversion of different image sources into the unified format, see **Figure 5a** and **b**. Further, this image layout is used to process the color spectrum of each individual variant, see **Figure 5c**. This enables the comparison of the color hue, saturation and color span of each particular variant.

## 5. CONCLUSIONS

A method to prepare self-similar patterns that present variation of structural colors was presented. Real samples were prepared using the e-beam lithography patterning. The samples exhibit large gamut of achievable colors. Ongoing work includes several topics related to the presented one.

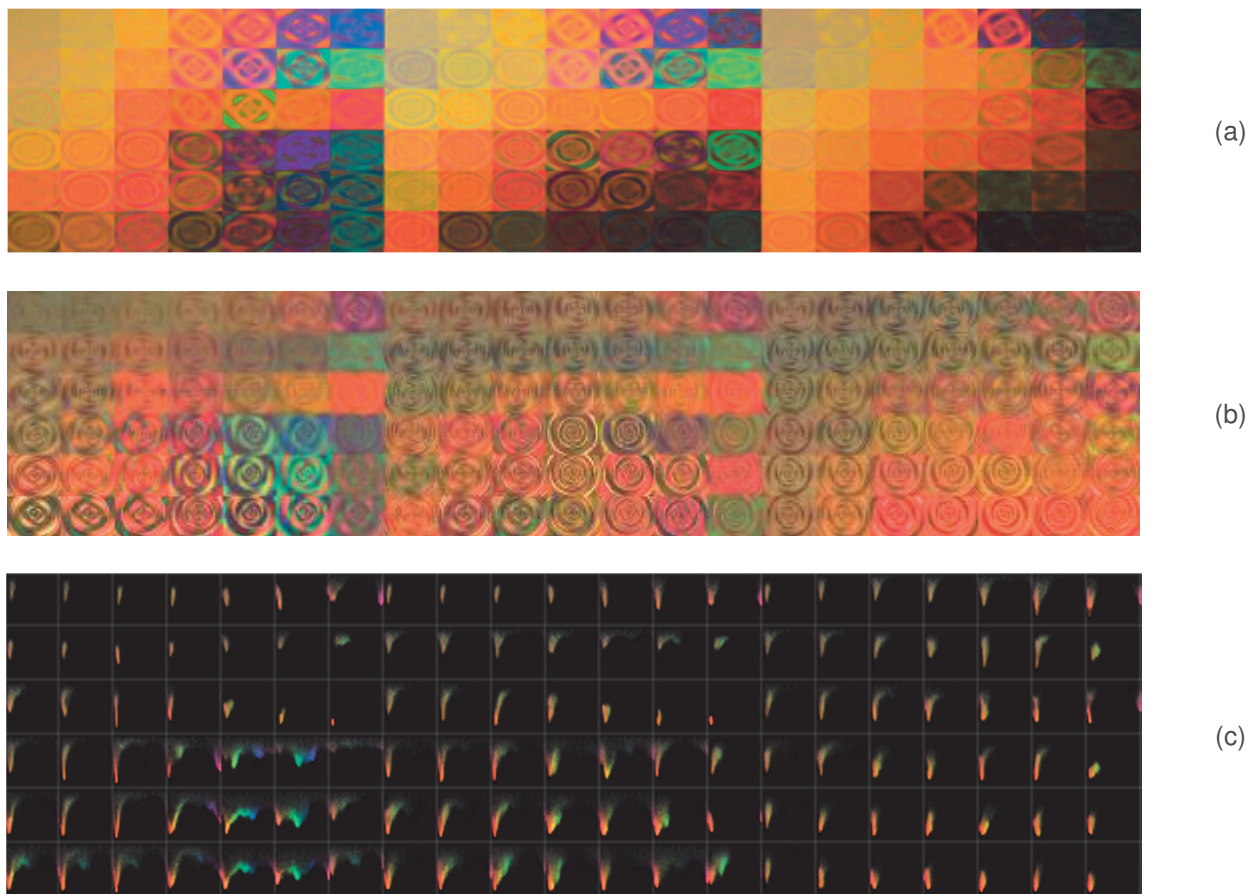


**Figure 5** Analysis of the sample 2 with sputtered Ag layer, positive-tone variants A1-F21: an overview photographic picture of the sample prepared for image processing (a); a set of 126 integrated micro photos prepared for image processing (b); a color spectra of the micro photo set (c)

## ACKNOWLEDGEMENTS

*The research was partially supported by the TACR project TE 01020233, by MEYS CR (LO1212), its infrastructure by MEYS CR and EC (CZ.1.05/2.1.00/01.0017) and by CAS (RVO:68081731).*

## REFERENCES

- [1] KOLAŘÍK, V. *et al.*, Structural Color of Metallic Surfaces. In *METAL 2014: 23rd International Conference on Metallurgy and Materials*. Ostrava: TANGER, 2014, pp. 962-967.
- [2] RENESSE, R. L. van, *Optical Document Security, 3rd edition*, Boston/London: Artech House (2005), 386 pages, ISBN 1-58053-258-6.
- [3] MELUZÍN, P. *et al.*, Some Other Gratings: Benchmarks for Large-Area E-Beam Nanopatterning. In *NANOCON 2014: 6th Int'l Conference Proceedings*. Ostrava: TANGER, 2014, pp. 246-251.
- [4] VOGEL, H., A better way to construct the sunflower head. *Mathematical Biosciences* 44 (1979): pp. 179-189.
- [5] HORÁČEK, M. *et al.*, Exposure Time Comparison between E-Beam Writer with Gaussian Beam and Variable Shaped Beam. In *NANOCON 2014: 6th Int'l Conference Proceedings*. Ostrava: TANGER, 2014, pp. 252-256.
- [6] ZDEBOROVÁ, L., Sunflower head and Fibonacci numbers. *Rozhledy matematicko-fyzikální* 82 (2007), no. 1, (in Czech), pp. 1-10.
- [7] KRÁTKÝ, S. *et al.*, PEC Reliability in 3D E-beam DOE Nanopatterning. *Microscopy and Microanalysis* 21 (2015), S4, pp. 230-235.